Spin-Reorientation, Ferroelectricity, and Magnetodielectric Effect in $YFe_{1-x}Mn_xO_3(0.1 \leq x \leq 0.40)$

P. Mandal, Venkata Srinu Bhadram, Y. Sundarayya, Chandrabhas Narayana, A. Sundaresan,* and C. N. R. Rao

Chemistry and Physics of Materials Unit, International Centre for Materials Science, Jawaharlal Nehru Centre for Advanced Scientific Research, Jakkur P.O., Bangalore 560 064 India

(Received 30 May 2011; revised manuscript received 17 July 2011; published 19 September 2011)

We report the observation of magnetoelectric and magnetodielectric effects at different temperatures in Mn-substituted yttrium orthoferrite, $YFe_{1-x}Mn_xO_3(0.1 \leq x \leq 0.40)$. Substitution of Mn in antiferromagnetic $YFeO_3(T_N = 640\ K)$ induces a first-order spin-reorientation transition at a temperature, T_{SR}, which increases with x whereas the Néel temperature (T_N) decreases. While the magnetodielectric effect occurs at T_{SR} and T_N, the ferroelectricity appears rather at low temperatures. The origin of magnetodielectric effect is attributed to spin-phonon coupling as evidenced from the temperature dependence of Raman phonon modes. The large magnetocapacitance (18% at 50 kOe) near $T_{SR} = 320\ K$ and high ferroelectric transition temperature ($\sim 115\ K$) observed for $x = 0.4$ suggest routes to enhance magnetoelectric effect near room temperature for practical applications.

DOI: 10.1103/PhysRevLett.107.137202 PACS numbers: 75.47.Lx, 75.85.+t, 77.84.−s, 78.30.−j

Demand of high efficiency memory devices has triggered a quest for new materials with various physical degrees of freedom coupled intimately. For example, the control of electric order parameter with a magnetic field and vice versa in a material would give rise to an extra degree of freedom in such device operation. In this context, magnetoelectric materials, wherein the electric or the magnetic dipole moment can be induced or modified by the application of an external magnetic or electric field, are of importance [1–5]. In particular, magnetoelectric multiferroic materials showing coupling between ferroelectric and ferro- or antiferromagnetic orders [3–7] have been demonstrated to be useful for new device applications [7,8]. Unfortunately, in most of the materials reported so far, the coupling is either weak and/or realized far below room temperature, which makes most of them inapplicable for practical usage. In magnetically induced multiferroic materials, the magnetoelectric effect manifests itself in terms of the occurrence of a polar state below a dielectric anomaly in the vicinity of a magnetic transition temperature [3–5]. In several systems, however, a dielectric anomaly is observed without the presence of spontaneous electric polarization, representing solely the magnetodielectric effect [9,10]. Such magnetodielectric materials can also have potential applications in microwave tunable filters, miniaturization of antenna, magnetic sensors, and spin-charge transducers [11].

The isostructural $SeCuO_3$ and $TeCuO_3$ compounds exhibit the magnetodielectric effect at ferromagnetic ($T_C = 25\ K$) and antiferromagnetic ($T_N = 9\ K$) transitions, respectively, due to spin-phonon coupling [9]. When a magnetic field is applied, a change in the capacitance is observed due to coupling between electric and magnetic orders. However, magnetocapacitance can also be observed due to the combined effect of the Maxwell-Wagner effect and magnetoresistance [12,13]. Therefore, it is important to separate out the intrinsic magnetocapacitance effect from the interfacial magnetocapacitance [12].

In this Letter, we report a novel case of the magnetodielectric effect across the magnetic transitions due to spin reorientation and antiferromagnetism in Mn-substituted $YFeO_3$. Further, we observe ferroelectric polarization at a temperature different from that of the magnetodielectric effect. The parent compound $YFeO_3$ is a canted antiferromagnet below the Néel temperature ($T_N = 640\ K$), due to the antisymmetric Dzyaloshinsky-Moriya interaction [14]. Upon Mn substitution at the Fe site, a spin-reorientation transition occurs at T_{SR} where the antiferromagnetic easy axis initially oriented along the a axis changes its direction to the b axis [15,16]. This transition is similar to the Morin transition observed in α-Fe_2O_3 near 260 K [17]. With increase of x in $YFe_{1-x}Mn_xO_3$, T_N decreases whereas T_{SR} increases and these two transitions occur close to 330 K for $x = 0.45$. Interestingly, we found a magnetodielectric effect at the first-order spin-reorientation transition as well as at the Néel temperature. A large magnetocapacitance of 18% (50 kOe) is observed for $x = 0.4$ near $T_{SR} = 317\ K$. Anomalies in the temperature dependent phonon modes associated with the Jahn-Teller distorted MnO_6 octahedra, as probed by Raman spectroscopy, indicated a spin-phonon coupling that could be the underlying mechanism for magnetodielectric effect in this system.

Phase pure polycrystalline samples of $YFe_{1-x}Mn_xO_3$ ($x = 0.1, 0.2, 0.3, 0.4$) were obtained by solid state route and details are described elsewhere [16]. Magnetic measurements were carried out with a vibrating sample magnetometer in a physical property measurement system (PPMS). Silver paint was applied on both sides of the

pellet and the capacitor was mounted in a custom made sample probe assembly which was then inserted in a 14 T cryo-cooled magnet system to collect temperature and magnetic field dependent data. Agilent 4294A impedance analyzer was used to study dielectric properties in the frequency range 100 Hz to 1 MHz by applying a small ac bias of 20 mV. Pyroelectric measurements were carried out using a Keithley 6517A electrometer. During this measurement the sample was poled down to lowest temperature and then shorted after removing the field to discharge any stray current. Pyroelectric current was measured while heating the sample at the rate of 4 K/min. Raman experiments were carried out in the backscattering geometry using custom built Raman equipment [18] with a 532 nm laser excitation from a frequency doubled Nd-YAG laser with the laser power of 8 mW at the sample. Temperature dependent studies were performed using a temperature-controller (Linkam TMS 94) equipped with a heating stage unit (Linkam THMS 600).

All the samples were single phase with the orthorhombic (space group: *Pnma*) structure as reported earlier [16]. In this space group, Fe and Mn ions are distributed in the same crystallographic (4*b*) site and therefore rules out the ordering of Fe and Mn ions. Our Mössbauer studies confirm that Fe ions are present in trivalent state [19]. The local Jahn-Teller distortion inferred from different Fe/Mn-O bond lengths and change in lattice parameters with x confirm that Mn ions are also present in trivalent state. We observe anomalies in the temperature dependence of dielectric constant near the magnetic transitions in $YFe_{1-x}Mn_xO_3$, which is a signature of magnetodielectric effect in these materials. Figure 1 shows the variation of dielectric constant (left axis) and field cooled (FC) magnetization data (right axis) with temperature for compounds with $x = 0.2$ and 0.3. Magnetodielectric behavior for the $x = 0.4$ sample is displayed in Fig. 2. It can be seen that the dielectric anomaly becomes pronounced at higher Mn-concentration. For $x = 0.1$, we could not detect any anomaly at T_{SR} indicating the important role of Mn in inducing magnetodielectric effect. The first-order spin-reorientation transition in the Mn-substituted yttrium orthoferrite, $YFe_{1-x}Mn_xO_3 (0 \leq x \leq 0.20)$ has also been investigated by ^{57}Fe Mössbauer spectroscopy. Analysis of the Mössbauer spectra confirms the occurrence of spin-reorientation relative to the crystal axes. At a given temperature, the mean hyperfine field decreases with increasing Mn concentration. The variation of canting angle with temperature could also be estimated [19].

For a detailed investigation of magnetodielectric effect at the magnetic transitions, we chose the composition with the maximum Mn content ($x = 0.4$), exhibiting spin reorientation close to room temperature. Figure 2(a) shows magnetization data for $x = 0.4$ recorded in field cooled warming (FCW) and field cooled cooling (FCC) modes (shown by arrows) under an applied field of 100 Oe. It can be seen that there is an irreversibility between the curves at $T_{SR} \sim 317$ K (100 Oe), confirming that the spin reorientation is a first-order transition whereas the antiferromagnetic transition at $T_N \sim 370$ K is of second order. Capacitance measurements show a steplike increase in dielectric constant above 250 K and an anomaly at T_{SR} [inset of *c* of Fig. 2(b)]. The large value of dielectric constant at room temperature (2500 at 1 kHz) and origin of the steplike increase will be discussed later. A dielectric anomaly is also seen at T_N (inset *d* of Fig. 2), indicating the magnetodielectric effect both at T_{SR} and T_N. To explore the magnetodielectric effect further, we have investigated the effect of the magnetic field on the spin-reorientation

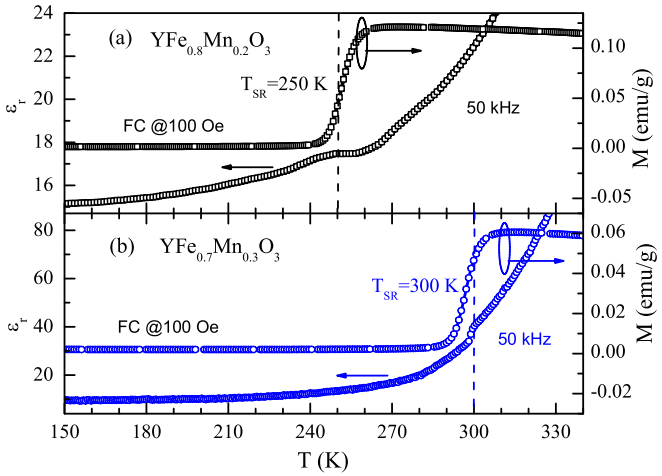

FIG. 1 (color online). Magnetodielectric effect in $YFe_{1-x}Mn_xO_3$. Dielectric constant (left axis) shows an anomaly near the reorientation transition in field cooled magnetization data (right axis) in compounds $YFe_{0.8}Mn_{0.2}O_3$ (upper panel *a*) and $YFe_{0.7}Mn_{0.3}O_3$ (lower panel *b*).

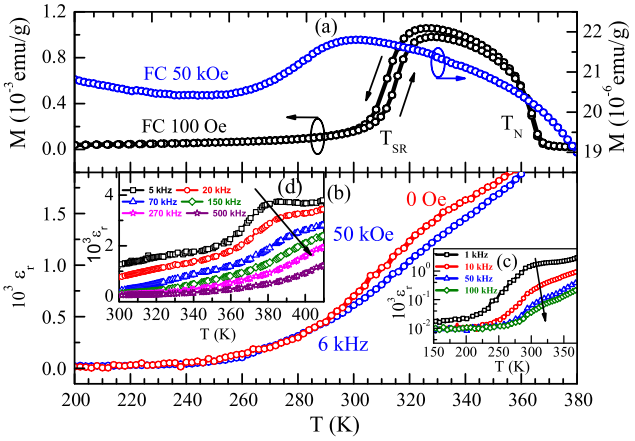

FIG. 2 (color online). Temperature dependence of (a) field cooled magnetization data under applied field of 100 Oe and 50 kOe showing change in the spin-reorientation temperature and (b) dielectric constant at 0 T and 50 kOe revealing a magnetocapacitance effect in $YFe_{0.6}Mn_{0.4}O_3$. The insets show dielectric constant anomalies near T_{SR} and T_N.

transition and dielectric constant. Increase of magnetic field not only reduces T_{SR} but suppresses the spin reorientation as it is induced by anisotropy of Mn^{3+} ions. As Fig. 2(a) demonstrates, at a high magnetic field (50 kOe) T_{SR} is decreased to 305 from 317 K at 100 Oe, indicating that the dielectric constant might be affected by the applied magnetic field. We, indeed, observe large effect (-25% at 6 kHz) near 320 K (Fig. 3) at 50 kOe with no significant shift in the dielectric constant. Because of the limitation of the magnetic field at high temperature, we could not measure magnetocapacitance at T_N. However, a magnetocapacitance of -5% at 50 kOe is observed at 360 K.

As mentioned before, the measured magnetocapacitance has both intrinsic and extrinsic origin. In order to estimate the intrinsic contribution to magnetocapacitance near T_{SR}, we have carried out temperature and frequency dependence of capacitance and loss. Before we discuss magnetocapacitance, it is important to understand the steplike increase of the dielectric constant and its high value. A large dielectric constant is observed in ferroelectric materials near the Curie temperature. In nonferroelectric materials, large dielectric constant values are observed due to polarization at grain boundaries or at the material-electrode interface known as Maxwell-Wagner effect [20]. As there is no magnetic anomaly at 250 K, the large value of dielectric constant in the present case may arise from Maxwell-Wagner effect. This was confirmed from the loss data which showed two peaks corresponding to different relaxations. The low temperature peak that corresponds to the steplike increase in dielectric constant, shifts towards high temperature with increasing frequency, confirms the presence of Maxwell-Wagner relaxation. Clearly, there is a contribution from the Maxwell-Wagner effect to the observed magnetocapacitance. The second peak at high temperature corresponds to the dielectric constant anomaly at 320 K, follows Debye relaxation. To estimate the extrinsic contribution due to the Maxwell-Wagner effect to the magnetocapacitance, we have analyzed magnetoresistance and the frequency dependence of magnetocapacitance and magnetoloss. In the Maxwell-Wagner model, the material under test can be considered as two parallel capacitance-resistance (C-R) circuits connected in series with one of the resistance in C-R circuits possibly having magnetically tunable resistance [12]. Consequently, a finite magnetoresistance can induce a magnetocapacitance effect which should not be attributed to magnetodielectric coupling. Intrinsic behavior can be observed at frequencies greater than the corresponding relaxation time ($f_0 = \tau_0^{-1} = \mathrm{RC}^{-1}$) below which the slow resistive processes contribute significantly to the dielectric response. Four-probe resistivity data showed a high value ($> 10^5\ \Omega$ cm) near room temperature indicating insulating behavior of the compound. A negligible magnetoresistance ($< -0.3\%$) was observed near the magnetic transitions even at a high field of 50 kOe whereas the corresponding magnetocapacitance value is -18% as shown in the inset of Fig. 3. Thus, the large magnetocapacitance observed by us cannot be explained in terms of small magnetoresistance.

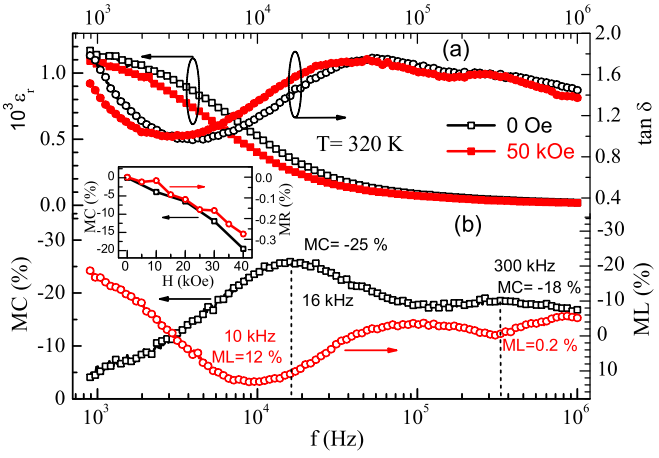

FIG. 3 (color online). (a) Top panel shows frequency dependence of dielectric constant (left axis) and loss (right axis) under 100 Oe and 50 kOe at 320 K. Bottom panel (b) shows magnetocapacitance (MC) and magnetoloss (ML) against frequency. Inset shows field dependence of magnetoresistance and magnetocapacitance. Large MC and low ML values at high frequency indicate intrinsic magnetodielectric behavior.

We have estimated the extrinsic and intrinsic contributions by analyzing the frequency dependence of magnetocapacitance and magnetoloss. As shown in Fig. 3(a), the real part of dielectric constant shows a fall with increasing frequency, which coincides with the peak in loss spectra (at 55 kHz). This behavior is indicative of a Debye-like relaxation process in a Maxwell-Wagner system. At 50 kOe of magnetic field, the dielectric constant value decreases with a corresponding shift in the loss peak to 44 kHz. Magnetocapacitance $\left(\mathrm{MC} = \left(\frac{C(H)-C(H=0)}{C(H=0)}\right) \times 100\right)$ value increases at low frequency taking a peak at 16 kHz and remains almost constant at high frequency ($f > \tau_0^{-1}$). On the other hand, magnetoloss $\left(\mathrm{ML} = \left(\frac{D(H)-D(H=0)}{D(H=0)}\right) \times 100\right)$; D = loss, changes from high negative value (-20%) at low frequency to a positive maximum value of 12% at 10 kHz whereas at very high frequency the magnetoloss value is small. An important feature to note is that at low frequency the maximum of magnetocapacitance and magnetoloss curves do not exactly coincide with each other which would be expected in the case where magnetocapacitance is completely driven by extrinsic effects. On the other hand, high frequency magnetocapacitance value is quite high (-18% at 300 kHz) where the corresponding magnetoloss is low (0.2%). At high frequency, Maxwell-Wagner relaxation related resistive processes do not respond and therefore the magnetocapacitance of -18% is intrinsic. The large magnetocapacitance arises due to the field dependent spin-reorientation transition where there is

a change in the magnetic structure that couples with the local lattice structure.

In order to explore whether the observed magnetodielectric effect at the magnetic transitions is accompanied by a ferroelectric order, we performed pyroelectric current measurements. Interestingly, the current shows a peak near 115 K for $x = 0.4$ both at negative and positive poling fields (inset of Fig. 4) that is an indication of para- to ferroelectric transition (T_C). It has been observed that the peak shifts to higher temperatures with decreasing x. Polarization for $x = 0.4$, obtained by integrating the pyroelectric current data, as shown in Fig. 4, confirms the bipolar nature of the compound. Though the polarization values observed in this system are small ($\sim 0.02\ \mu C/cm^2$) they are comparable to those reported for related materials [3–5]. It is important to note the effect of magnetic field on the ferroelectric polarization. As seen in Fig. 4, the polarization increases with applied filed, indicating a substantial magnetoelectric coupling. Further, with increasing field the ferroelectric transition shifts to low temperature, which indicates the relevance of spin-phonon coupling to the physical origin of ferroelectricity. It should be noticed that the polarization appears at a temperature much below the magnetic transitions where the magnetodielectric effect occurs, which implies that ferroelectricity and magnetodielectric effect may not have a common origin. In magnetically induced multiferroic materials, the ferroelectric transition is reflected as an anomaly in magnetization, dielectric constant and heat capacity data. In the present system, we do not see any such anomaly but observe a sudden change in Raman phonon modes near the ferroelectric transition, indicating the relevance of spin-phonon coupling to the origin of ferroelectricity. However, it requires a detailed neutron diffraction study around the ferroelectric transition as certain types of noncollinear magnetic structure has been attributed to the origin of ferroelectricity in magnetically induced magnetoelectric materials [3–5].

Raman spectroscopic measurements have been carried out across the magnetic and ferroelectric transitions in $YFe_{0.6}Mn_{0.4}O_3$.Unpolarized Raman spectrum recorded at room-temperature is shown in Fig. 5(a). Lattice dynamical calculations have predicted 24 Raman active modes in the orthorhombic perovskites [21]. The mode assignment corresponding to various vibrational symmetries is shown in Fig. 5(a). Deconvolution of the strongest Raman feature centered at 640 cm^{-1} shows two prominent bands at 624 and 648 cm^{-1} corresponding to B_{3g} and B_{2g} symmetries. Since it is observed that these modes are weak in $YFeO_3$ and are intense in $RMnO_3$ systems [21,22], we attribute these modes to the out-of-phase and in-phase stretching of Jahn-Teller distorted MnO_6 octahedra, respectively. The temperature dependence of the frequencies of modes at 624 and 648 cm^{-1} around the ferroelectric and magnetic transitions are shown in Figs. 5(b) and 5(c), respectively. For a general case, the temperature dependence of phonon frequency $\omega(T)$, follows the relation $\omega(T) = \omega_0 - C(1 + (2/e^{(\hbar\omega_0/2K_BT)} - 1))$ which describes solely the anharmonic phonon-phonon scattering. In the present case, the temperature dependence of both B_{2g} and B_{3g} modes deviates from the above relation at T_C, T_N and T_{SR}. These modes display subtle hardening at T_N, softening across T_{SR} and a sudden increase in phonon frequency at T_C. These anomalous behavior is attributed to spin-phonon coupling caused by the phonon modulation of

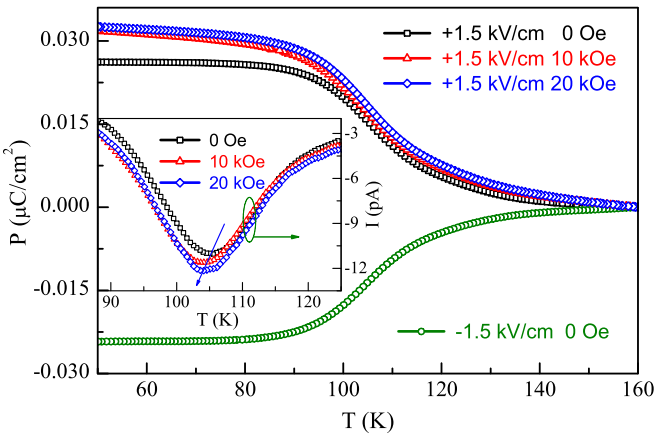

FIG. 4 (color online). Temperature dependence of ferroelectric polarization, P in $YFe_{0.6}Mn_{0.4}O_3$ at positive and negative poling fields confirming bipolar nature. Polarization is observed to increase with magnetic field with a corresponding decrease in the Curie temperature. Inset shows the effect of magnetic field on the ferroelectric transition temperature.

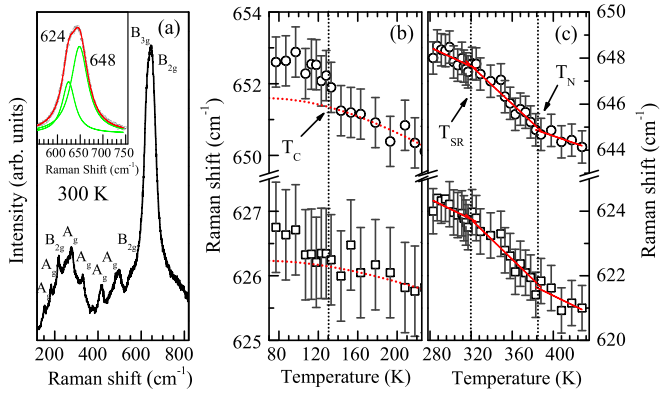

FIG. 5 (color online). (a) Raman spectrum of $YFe_{0.6}Mn_{0.4}O_3$ recorded at room temperature. Inset shows the deconvoluted peak centered around 640 cm^{-1} into B_{2g} and B_{3g} modes. Temperature dependence of frequency corresponding to B_{2g} and B_{3g} phonon modes across the (b) ferroelectric and (c) magnetic transitions (see text for details). Solid lines in (c) are guide to eye and dotted lines in (b) represent the anharmonic contributions.

spin exchange integral [23]. Furthermore, the FWHM of the phonon modes increases below T_{SR} and T_C (data is not shown), which indicates that there is a decrease in the lifetime of the phonons due to spin-phonon coupling. These results suggest that the spin-phonon coupling is involved in magnetodielectric effect and ferroelectricity.

In conclusion, we have demonstrated the occurrence of the magnetodielectric effect and the ferroelectricity at different temperature scales in Mn-substituted yttrium orthoferrite. The large magnetocapacitance observed at the spin-reorientation transition near room temperature is intrinsic and originates from spin-phonon coupling. The spin-phonon coupling is also reflected near the ferroelectric ordering at low temperature.

*sundaresan@jncasr.ac.in

[1] F. Manfred, J. Phys. D **38**, R123 (2005).
[2] W. Eerenstein, N. D. Mathur, and J. F. Scott, Nature (London) **442**, 759 (2006).
[3] S. W. Cheong and M. Mostovoy, Nature Mater. **6**, 13 (2007).
[4] T. Kimura, Annu. Rev. Mater. Res. **37**, 387 (2007).
[5] Y. Tokura and S. Seki, Adv. Mater. **22**, 1554 (2010).
[6] D. I. Khomskii, J. Magn. Magn. Mater. **306**, 1 (2006).
[7] V. Laukhin *et al.*, Phys. Rev. Lett. **97**, 227201 (2006).
[8] Y. H. Chu *et al.*, Nature Mater. **7**, 478 (2008).
[9] G. Lawes *et al.*, Phys. Rev. Lett. **91**, 257208 (2003).
[10] R. Tackett *et al.*, Phys. Rev. B **76**, 024409 (2007).
[11] Y. S. Shin and S. O. Park, Microw. Opt. Technol. Lett. **52**, 2364 (2010).
[12] G. Catalan, Appl. Phys. Lett. **88**, 102902 (2006).
[13] T. Bonaedy *et al.*, Appl. Phys. Lett. **91**, 132901 (2007).
[14] D. Treves, Phys. Rev. **125**, 1843 (1962).
[15] Y. Nagata and K. Ohta, J. Phys. Soc. Jpn. **44**, 1148 (1978).
[16] P. Mandal *et al.*, private communication (2011).
[17] F. J. Morin, Phys. Rev. **78**, 819 (1950).
[18] G. V. P. Kumar and C. Narayana, Curr. Sci. **93**, 778 (2007), http://www.ias.ac.in/currsci/sep252007/778.pdf.
[19] Y. Sundarayya *et al.*, private communication (2011).
[20] P. Lunkenheimer *et al.*, Phys. Rev. B **66**, 052105 (2002).
[21] M. N. Iliev *et al.*, Phys. Rev. B **57**, 2872 (1998).
[22] J. Laverdière *et al.*, Phys. Rev. B **73**, 214301 (2006).
[23] E. Granado *et al.*, Phys. Rev. B **60**, 11 879 (1999).